



HAL
open science

Effect of fines content on soil freezing characteristic curve of sandy soils

Quoc Hung Vu, Jean-Michel Pereira, Anh Minh Tang

► **To cite this version:**

Quoc Hung Vu, Jean-Michel Pereira, Anh Minh Tang. Effect of fines content on soil freezing characteristic curve of sandy soils. *Acta Geotechnica*, 2022, 17 (11), pp.4921-4933. 10.1007/s11440-022-01672-9 . hal-04375134

HAL Id: hal-04375134

<https://enpc.hal.science/hal-04375134>

Submitted on 5 Jan 2024

HAL is a multi-disciplinary open access archive for the deposit and dissemination of scientific research documents, whether they are published or not. The documents may come from teaching and research institutions in France or abroad, or from public or private research centers.

L'archive ouverte pluridisciplinaire **HAL**, est destinée au dépôt et à la diffusion de documents scientifiques de niveau recherche, publiés ou non, émanant des établissements d'enseignement et de recherche français ou étrangers, des laboratoires publics ou privés.

1 Effect of fines content on soil freezing characteristic curve of
2 sandy soils

3 Quoc Hung VU, Jean-Michel PEREIRA, Anh Minh TANG

4 Laboratoire Navier, Ecole des Ponts, Univ Gustave Eiffel, CNRS, Marne-la-Vallée, France

5

6

7

8

9 Corresponding author:

10 Dr. Anh Minh TANG

11 Research Director

12 Ecole des Ponts ParisTech

13 6-8 avenue Blaise Pascal

14 77455 Marne-la-Vallée

15 France

16 Email: anh-minh.tang@enpc.fr

17

18

19 **Abstract:** Soil freezing characteristic curve (SFCC) represents the relationship between soil
20 temperature and unfrozen water content of soil during freezing and thawing processes. In this
21 study, SFCC of sandy soils was determined in laboratory. Pure sand was mixed with clay at
22 various contents (0, 5, 10, 15, and 20% of the total dry mass) and the mixtures were
23 compacted to their respective maximum dry density. Compacted specimens were then placed
24 in a close and rigid cell and the soil's temperature was decreased step-by-step to freeze the
25 soil water and then increased back to thaw it. During this thermal cycle, soil's temperature
26 and volumetric water content were monitored in order to determine the SFCC. The results
27 show that SFCC was strongly dependent on the fines content: at higher fines content, the
28 temperature of spontaneous nucleation was lower and the residual unfrozen volumetric water
29 content was higher.

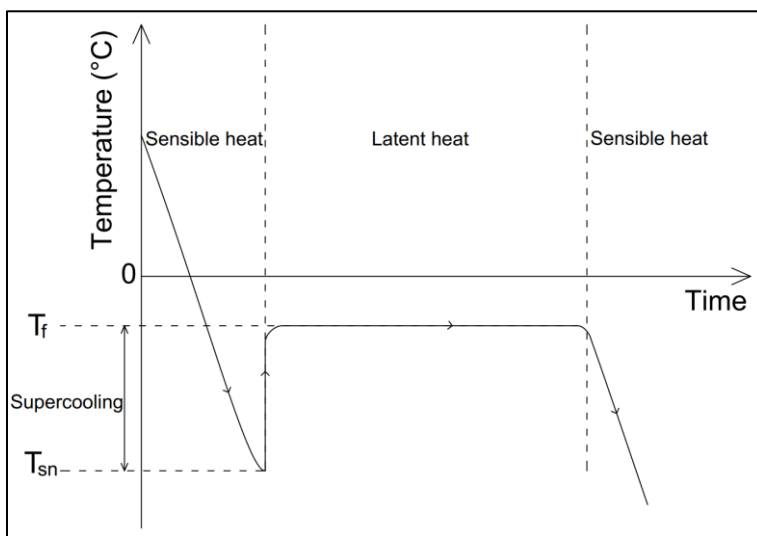
30 **Keywords:** temperature of spontaneous nucleation, hysteresis, soil freezing characteristic
31 curve, residual water content.

32 **1. Introduction**

33 Frozen soil consists of mineral particles, liquid water, ice and gas. It is formed from unfrozen
34 soil during freezing, when a fraction of liquid water solidifies into ice at temperatures
35 sufficiently low below 0 °C [1]. This phase change causes significant modifications of
36 physical-hydraulic-mechanical properties of soils [2]. The freezing-thawing process is
37 encountered in cold regions, seasonal cold regions as well as construction works using
38 artificial ground freezing technique. Two main consequences of this process that need to be
39 mentioned are frost heave and thaw settlement. These phenomena can induce damages to
40 infrastructure [3–6].

41 The freezing-thawing process in porous media has been investigated not only in civil
42 engineering and geosciences but also in physics [7–11]. While bulk water melts at 0 °C, water
43 in porous media melts at temperatures below 0 °C because of physical interactions between
44 water and solid particles [12–14]. Freezing process of a soil sample (where heat is extracted
45 from the sample with a constant rate) can be divided into three steps (as shown in Fig. 1): (i)
46 supercooling with release of sensible heat; (ii) first water freezing with release of latent heat;
47 (iii) further water freezing with release of sensible heat. In the first step, during cooling
48 (extraction of heat from soil), soil temperature decreases to reach a certain value from that it
49 cannot decrease anymore. This value is called temperature of spontaneous nucleation T_{sn}

50 where the first ice embryo nucleus forms because it attains the critical size [15, 16].
 51 Formation of ice crystals releases latent heat and thus increases soil temperature. From T_{sn} ,
 52 soil temperature increases to reach another value which is called freezing temperature T_f ,
 53 where it remains on a plateau for a while. During this second step, soil water is gradually
 54 frozen along with releasing latent heat. After that, within the third step, soil temperature
 55 decreases with further water freezing. Freezing temperature T_f , also considered to be equal to
 56 thawing temperature T_t at which soil state changes from frozen to unfrozen, is usually used as
 57 a boundary value index to distinguish between frozen soil and unfrozen soil [17–19]. These
 58 characteristic temperatures (T_{sn} and T_f) were investigated in several studies [15, 18, 20].



59

60 **Fig. 1** Freezing process of soil-water system.

61 Soil freezing characteristic curve (SFCC) represents the relationship between the temperature
 62 and the quantity of liquid water in soil. It is one of the most essential data in studying the
 63 freezing-thawing process in soils. On the one hand, several SFCC models were empirically
 64 developed. From SFCC obtained experimentally, empirical models were proposed using
 65 power, piecewise or exponential functions [21–28]. On the other hand, SFCC can be derived
 66 from soil water characteristic curve (SWCC). This approach is based on the theory of
 67 similarity between freezing-thawing and drying-wetting processes that is illustrated by
 68 Clapeyron equation [29–37]. More generally, various physical models were developed based
 69 on theory of capillarity, sorption or that of interface pre-melting [38–40]. Most of the existing
 70 SFCC models consider the effect of fines content but this effect is considered in different
 71 ways. For instance, some empirical models used specific surface or liquid limit as input data
 72 while physics-based models consider absorption parameters of soil. Due to the diversity of

73 SFCC models, there is no unified standard for choosing SFCC in numerical simulations [41].
74 In addition, except few models (e.g., [35]), most of the existing ones consider a unique
75 relationship between unfrozen water content and temperature. However, this relation obtained
76 on the freezing path can differ from that of that of the thawing path; at a given temperature,
77 water content of the freezing path can be higher than at of the thawing path. This hysteresis is
78 usually ignored in the models.

79 To determine SFCC in the laboratory, a soil specimen is usually subjected to a freeze-thaw
80 cycle, while unfrozen water content is measured. Although controlling specimen's
81 temperature is technically feasible, measuring unfrozen water content is much more
82 challenging. Several methods and techniques have been developed to evaluate the unfrozen
83 water content at negative temperature, including dilatometry [42, 43], gas dilatometry [44],
84 adiabatic calorimetry [45, 46], isothermal calorimetry [28], differential scanning calorimetry
85 [10, 47, 48], X-ray diffraction [49, 50], time/frequency domain reflectometry (TDR/FDR)
86 [51–53] and pulsed nuclear magnetic resonance (P-NMR) [38, 54, 55]. Among these methods,
87 TDR and P-NMR are the two most common ones. P-NMR is widely acknowledged as a
88 highly accurate and non-destructive technique. However, the equipment required for this
89 technique is generally expensive [56]. Compared to P-NMR, TDR/FDR can be used in the
90 laboratory as well as in the field and it is cheaper, quicker, and more portable. With TDR,
91 unfrozen water content is inferred from the measurement of apparent dielectric constant of
92 soil using an empirical equation [57, 58] or dielectric mixing models [51, 59, 60]. It is noted
93 that several factors such as temperature or bound water can affect its accuracy.

94 Several studies have determined SFCC in the laboratory in both freezing and thawing
95 processes [18, 40, 42, 55, 61–64]. These studies recognized that hysteresis exists in SFCC in
96 which the unfrozen water content is different in thawing and freezing processes at the same
97 temperature. Hysteresis in freezing-thawing process was believed to be similar to that of
98 wetting-drying process. However, the mechanism inducing hysteresis in SFCC is complex
99 and it may be influenced by several effects such as supercooling, pore blocking, capillarity,
100 free energy barriers, contact angles and electrolytes [55, 62]. It is also noted that hysteresis is
101 significant at temperatures between $-2\text{ }^{\circ}\text{C}$ and $0\text{ }^{\circ}\text{C}$ [42, 65, 66] and that it should not be
102 ignored due to impacts on unfrozen water content on frost heaving [67, 68], creep behaviour
103 of frozen soils [69, 70] as well as thermal regime of frozen ground [71].

104 Beside hysteresis effect, it is found that the shape of SFCC depends also on several factors,
105 including liquid limit [28], stress condition [72], salt content and solute types [38, 73], initial
106 water content or degree of saturation [74–76], types of soil [18, 62, 65], pore-size distribution
107 [55], and fines content [18, 28, 55, 63]. Among these factors, fines content can influence
108 others (liquid limit, pore-size distribution and types of soil). As far as fines content is
109 concerned, by determining unfrozen water content of several clays, a silt and a gravel, Tice et
110 al. [28] observed significantly different unfrozen water contents at the same temperature
111 below 0 °C. Tian et al. [63] carried out tests on three soils corresponding to three clay
112 contents and found that unfrozen water degree of saturation also changed in different ways in
113 both freezing and thawing processes. For soils containing higher clay fraction, unfrozen water
114 degree of saturation was higher at any given temperature below freezing point and the
115 hysteresis loop was smaller. The same findings concerning SFCC were obtained in the study
116 of Zhang et al. [18] on silty clay, and silt and in the study of Li et al. [55] on silty clay, fine
117 sand, and medium sand. Some other authors also investigated different soils but the effect of
118 fines content was out of their focus [22, 30, 54, 62].

119 The present study aims at systematically investigating the effect of fines content on the SFCC
120 of sandy soils. Clean sand was mixed with clay at dry state firstly and water afterward to
121 obtain sandy soils with clay content of 0, 5, 10, 15, and 20% prior to compaction at the
122 Proctor maximum dry density followed by a saturation phase. The specimen's temperature
123 was then decreased progressively to freeze the soil specimen in undrained conditions prior to
124 applying the thawing process. During this freezing-thawing cycle, soil's temperature and
125 unfrozen water content were measured. After the introduction, the second section of this paper
126 presents the materials and experimental methods. Experimental results are presented in the
127 third section, before being discussed in the fourth section.

128 **2. Materials and experimental methods**

129 **2.1. Experimental setup**

130 The experimental setup is shown in Fig. 2 and the details of the sensors used are presented in
131 Table 1. Soil specimen was contained in a rigid metallic cylindrical cell (150 mm in height
132 and 150 mm in diameter). The cell was immersed in a temperature-controlled bath (F38-EH
133 JULABO with ± 0.03 °C accuracy). Soil temperature was measured with a PT100 sensor, soil
134 volumetric water content was measured with a ML2x Thetaprobe sensor, and soil suction was

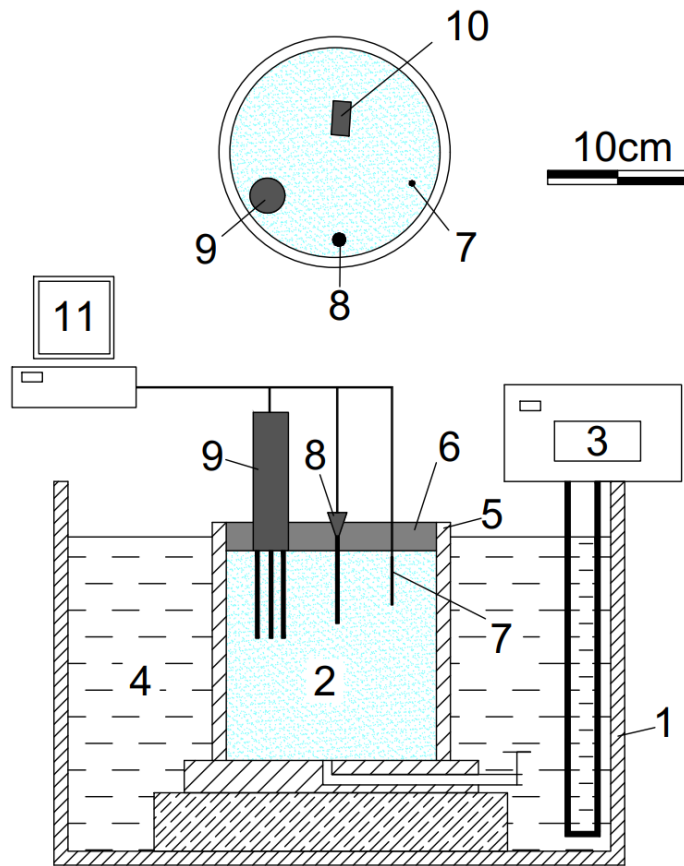
135 measured with a tensiometer. As Thetaprobe sensor measures soil apparent dielectric constant
 136 (K_a) which is the ratio of the dielectric permittivity of a substance to free space, soil unfrozen
 137 volumetric water content (θ_u) was estimated from measured K_a by using empirical equations
 138 of Smith and Tice [58] (1) and Topp et al. [57] (2) for frozen and unfrozen states of soil,
 139 respectively. Equation (2) was used only for the initial state (before the occurrence of
 140 freezing) and for the final state where thawing is complete. Equation (1) is used where ice is
 141 expected to exist in soil (i.e. after the occurrence of freezing and before the completion of
 142 thawing).

$$\theta_u = -0.1458 + 3.868 \times 10^{-2} \times K_a - 8.502 \times 10^{-4} \times K_a^2 + 9.92 \times 10^{-6} \times K_a^3 \quad (1)$$

$$\theta_u = -5.3 \times 10^{-2} + 2.92 \times 10^{-2} \times K_a - 5.5 \times 10^{-4} \times K_a^2 + 4.3 \times 10^{-6} \times K_a^3 \quad (2)$$

143 Table 1: Properties of sensors using in freezing-thawing tests.

Measured parameters	Principle	Type	Accuracy	Range
Temperature	Resistance temperature detector	PT100	± 0.03 °C	-200 to 400 °C
Volumetric unfrozen water content	Time domain reflectometry (dielectric constant)	ThetaProbe ML2x (4 rods)	0.01 m ³ /m ³	0.01 to 1 m ³ /m ³
Tensiometer	Piezoelectric transducer	T5x	± 0.5 kPa	-160 to 100 kPa
Thermal conductivity	Transient line heat source	KD2-Prob (RK-1)	10%	0.1 to 4 W/(m.K)



144

145 **Fig. 2** Schematic view of the experimental setup. (1) Temperature-controlled bath; (2) Soil
 146 specimen; (3) Temperature controlling system; (4) Temperature-controlled liquid (30%
 147 ethylene glycol + 70% water); (5) Metallic cylindrical cell; (6) Insulating cover; (7)
 148 Temperature sensor; (8) Tensiometer; (9) Soil water sensor; (10) Thermal conductivity probe
 149 (results are not presented in this study); (11) Data logger system.

150 2.2. Material

151 Fontainebleau sand was carefully mixed with Speswhite kaolin clay at dry state using an
 152 automatic mortar mixer in order to obtain sandy soils with fines content (dry mass of clay
 153 divided by dry mass of soil) of 0, 5, 10, 15, and 20%. The physical properties of sand and clay
 154 are shown in Table 2 and Table 3, respectively. Fig. 3 presents the grain size distribution of
 155 these soils. In this study, the name of each soil corresponds to its clay content (for instance,
 156 S10 corresponds to a soil having 10% of clay in dry mass). Prior to the preparation of the soil
 157 specimens, each soil was carefully mixed with distilled water using the mortar mixer to obtain
 158 optimum water content (determined from the Normal Proctor compaction curves obtained on
 159 the same soils [77]). Afterward, wet soil was packed in a plastic bag for at least 24 h to ensure

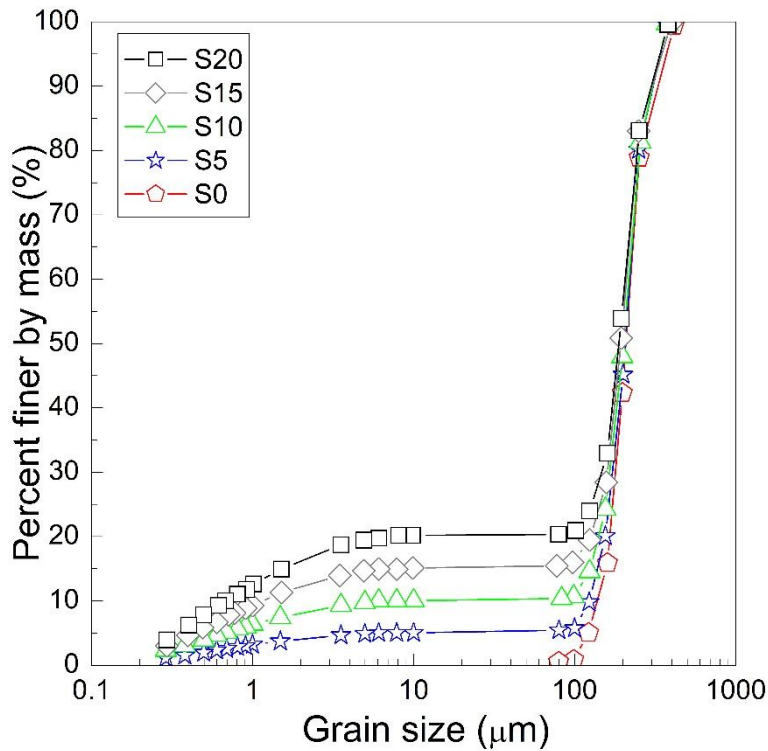
160 the homogenisation of water content, prior to compaction in the cylindrical cell to reach its
161 maximum dry density.

162 Table 2. Physical properties of sand.

Property	Value
Median grain size, D_{50} (mm)	0.21
Uniformity coefficient, C_U	1.52
Minimum void ratio, e_{min}	0.54
Maximum void ratio, e_{max}	0.94
Particle density, ρ_s (Mg/m³)	2.65
Minimum dry density, $\rho_{d,min}$ (Mg/m³)	1.37
Maximum dry density, $\rho_{d,max}$ (Mg/m³)	1.72

163 Table 3: Physical properties of clay.

Property	Value
Liquid limit, LL (%)	55
Plastic limit, PL (%)	30
Plasticity index, PI	25
Specific surface area (m²/g)	0.94
Particle density, ρ_s (Mg/m³)	2.65
Particle diameter < 0.002 mm (%)	79
Particle diameter > 0.01 mm (%)	0.5
Maximum dry density, $\rho_{d,max}$ (Mg/m³)	1.45



164

165 **Fig. 3** Grain size distribution curves.

166 **2.3. Experimental procedure**

167 After soil compaction in the cell, sensors were installed as shown in Fig. 2 and an insulating
 168 cover made of expanded polystyrene was placed in order to avoid heat exchange between soil
 169 specimen and ambient air. The whole system was then transferred inside the temperature-
 170 controlled bath. Prior to the freezing-thawing test, soil specimen was saturated by injecting
 171 water from the bottom of the specimen during 0.5 to 2 days depending on fines content. After
 172 the saturation (when a layer of water of 10 mm was visible on the top of the specimen), the
 173 temperature of the bath was first set at a temperature between 0 °C and -1 °C (slightly higher
 174 than the expected T_{sn}). Each test started with the cooling path. The bath temperature was
 175 decreased in steps of 0.1 °C to freeze the soil pore water. Once the freezing was triggered, the
 176 temperature continued to be decreased in steps of 0.2 °C until -2 °C or -3 °C to observe the
 177 change of liquid water content during further cooling. Afterward, during the heating path, the
 178 bath temperature was increased in steps of 0.2 °C until 0 °C to thaw the frozen soil. During
 179 both cooling and heating paths, the bath temperature was changed to the subsequent step only
 180 when soil temperature and volumetric unfrozen water content (measured by the sensors) had
 181 reached their equilibrium state. The equilibrium state was considered reached when these two

182 quantities did not change (< 0.05 °C for temperature and $< 1\%$ for water content) during at
183 least 2 h.

184 The test program is shown in Table 4. The test number shows the soil tested (S0 to S20)
185 followed by the number of replicate test (T1 to T4). At least two tests were performed for
186 each soil. Tests T1 were performed following the procedure described above to obtain the
187 complete SFCC curves. For the other tests (T2, T3, T4), only the freezing path of the same
188 procedure was performed in order to replicate the characteristic temperatures.

189 Table 4: Physical properties of soils.

Test No.	Fines content (%)	Dry density (Mg/m ³)	Porosity (-)	Test duration (h)
S20-T1	20	1.98	0.25	754
S20-T2	20	1.96	0.26	26
S15-T1	15	1.99	0.25	712
S15-T2	15	2.00	0.25	64
S10-T1	10	1.91	0.28	590
S10-T2	10	1.90	0.28	153
S5-T1	5	1.78	0.33	817
S5-T2	5	1.78	0.33	143
S5-T3	5	1.78	0.33	190
S0-T1	0	1.67	0.37	756
S0-T2	0	1.67	0.37	286
S0-T3	0	1.67	0.37	75
S0-T4	0	1.68	0.37	187

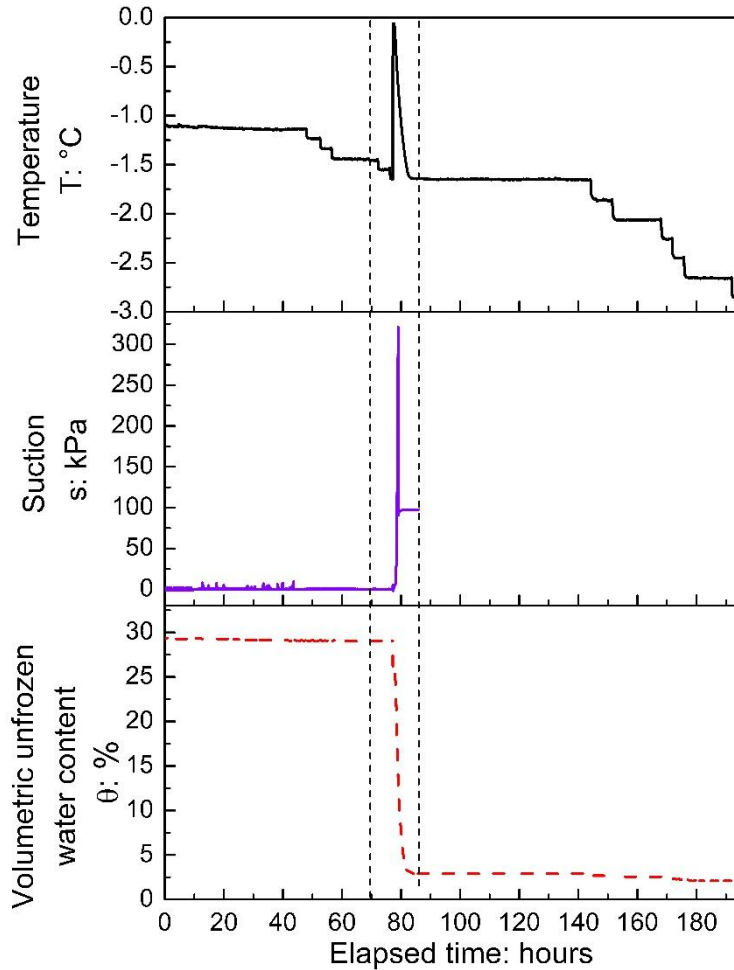
190 3. Experimental results

191 3.1. Typical test (S10-T1)

192 As an example, the results of test S10-T1 are shown in Fig. 4 where soil temperature, suction,
193 and volumetric unfrozen water content are plotted versus elapsed time for the cooling path.

194 From -1.2 °C, soil temperature was decreased in steps of 0.1 °C down to -1.6 °C. During this
195 period, soil temperature was controlled through the bath's temperature, suction remained

196 equal to zero and volumetric water content remained constant. When soil temperature reached
 197 $-1.6\text{ }^{\circ}\text{C}$, soil freezing started inducing abrupt changes in the three measured quantities. Results
 198 obtained during this stage (elapsed time of 70 – 86 h) are shown in Figure 5 for a better view.



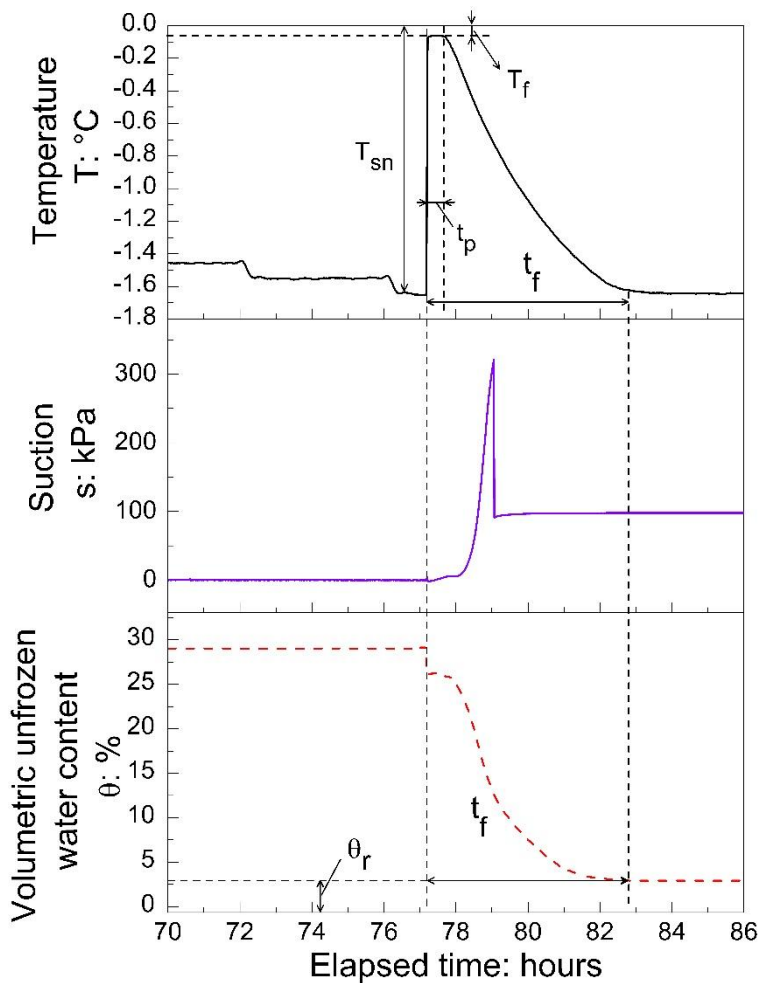
199

200 **Fig. 4** Soil temperature, volumetric unfrozen water content and suction versus elapsed time
 201 during the cooling path of test S10-T1.

202 As shown in Fig. 5, when the bath temperature was changed from $-1.5\text{ }^{\circ}\text{C}$ to $-1.6\text{ }^{\circ}\text{C}$ (at 76 h),
 203 soil temperature changed to $-1.6\text{ }^{\circ}\text{C}$ after a few minutes. At 77 h, while the bath temperature
 204 was still maintained at $-1.6\text{ }^{\circ}\text{C}$, soil temperature increased abruptly to $-0.1\text{ }^{\circ}\text{C}$ prior to a
 205 progressive decrease and reached the imposed temperature ($-1.6\text{ }^{\circ}\text{C}$) again at 83 h. Soil
 206 suction started to increase at 78 h and reached a maximum value of 300 kPa prior to fall down
 207 to 100 kPa. At 77 h, soil water content decreased abruptly from 28% to 26% prior to decrease
 208 progressively to 3 % at 82 h. These results are representative of a freezing process in soil (Fig.
 209 1) where the phase before 77 h corresponds to the supercooling step. At 77 h, soil water
 210 started to freeze: soil temperature increased abruptly because of latent heat release prior to

211 decrease because of heat diffusion toward the liquid surrounding the cell; soil suction
 212 increased quickly because of the cryogenic suction induced by ice formation in the pore space
 213 (the sudden decrease of suction from 300 kPa to 100 kPa corresponded to the cavitation of the
 214 tensiometer, after this moment, the sensor did not provide anymore the real soil suction);
 215 volumetric water content decreased because of ice formation. From these typical results, the
 216 following parameters were defined to characterise the freezing process (see Figure 5): (i)
 217 temperature of spontaneous nucleation, T_{sn} ; (ii) freezing point, T_f ; (iii) residual volumetric
 218 unfrozen water content, θ_r (the value recorded at temperature equal to T_{sn}); (iv) duration of
 219 the temperature plateau, t_p ; (v) duration of the freezing process, t_f .

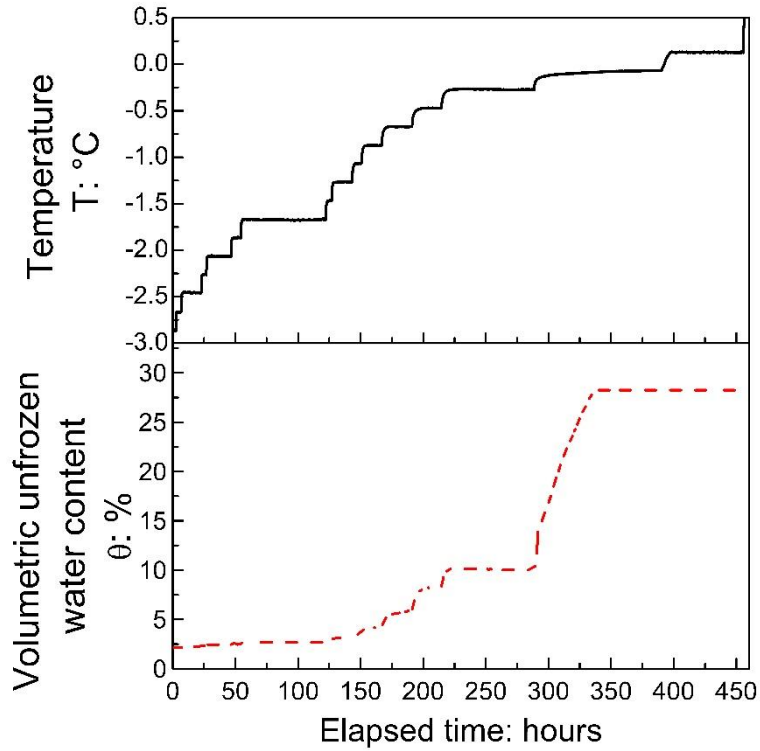
220 After the freezing process (from 83 h), decrease of temperature induced slight decrease of
 221 volumetric unfrozen water content (see Figure 4) while soil suction measurement was no
 222 longer available because of the cavitation of the tensiometer.



223

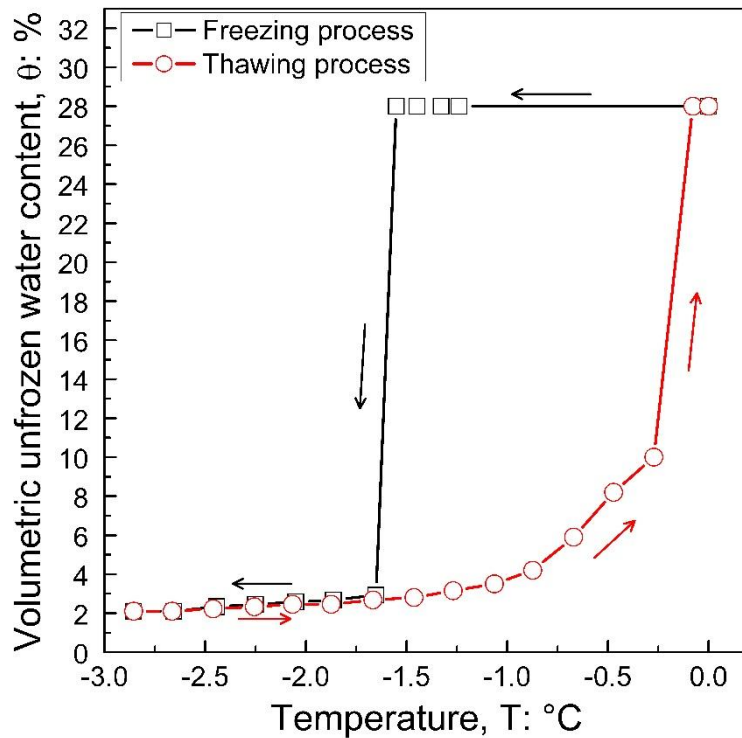
224 **Fig. 5** Soil temperature, volumetric unfrozen water content and suction versus elapsed time
 225 during the freezing process of test S10-T1 (detailed view from 70h to 86 h).

226 Fig. 6 shows the results of test S10-T1 during the heating path. During this path, temperature
227 was increased by steps of 0.2 °C from -2.8 °C to 0 °C. It induced thawing of frozen water
228 (corresponding to a gradual increase of unfrozen water content).



229
230 **Fig. 6** Soil temperature and volumetric unfrozen water content versus elapsed time during the
231 heating path of test S10-T1.

232 From the results shown in Fig. 4, Fig. 5 and Fig. 6, volumetric unfrozen water content
233 obtained at the end of each step is plotted versus the corresponding soil temperature for test
234 S10-T1 in Fig. 7. These results correspond to the SFCC of soil S10 obtained from test S10-
235 T1, which include both freezing and thawing paths.



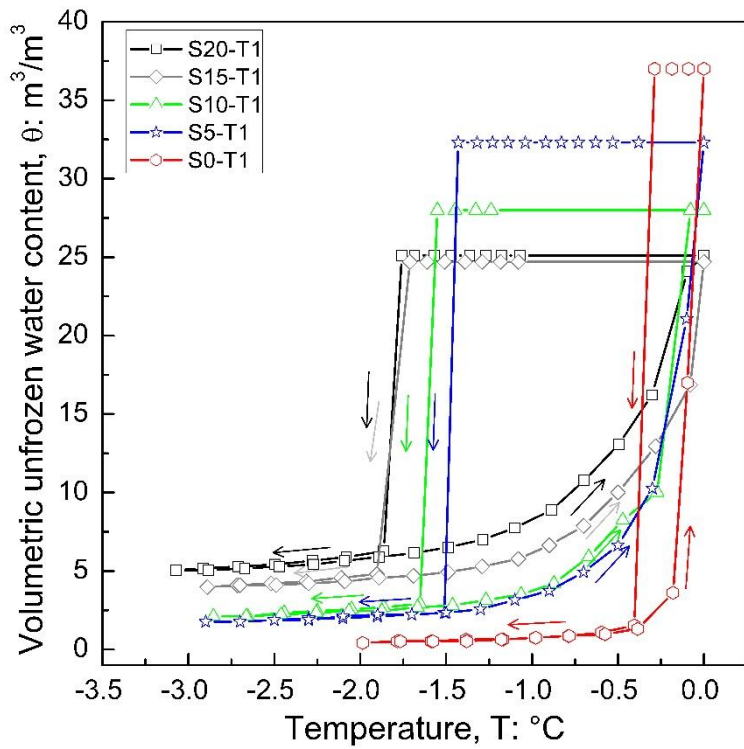
236

237 **Fig. 7** Soil freezing characteristic curve determined from test S10-T1.

238 **3.2. Effects of fines content**

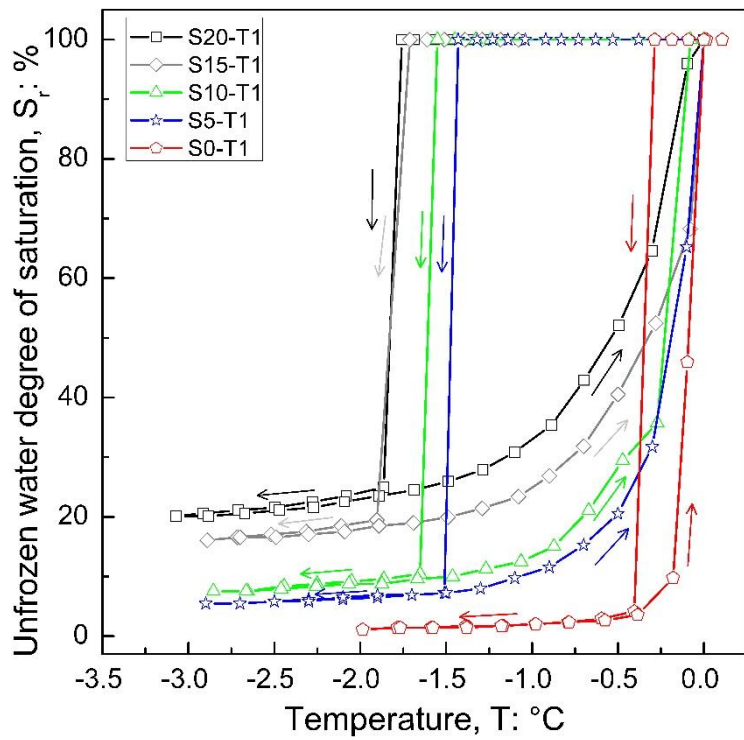
239 SFCC of all soils are shown in Fig. 8 where volumetric unfrozen water content was plotted
 240 versus temperature. As the initial volumetric water content (which depends on soil dry
 241 density) was different from one soil to the others, it is thus difficult to analyse the effect of
 242 fines content from these results. For this reason, volumetric unfrozen water content was used
 243 to calculate unfrozen water degree of saturation ($S_r = \theta / \theta_{sat}$; where θ_{sat} is the volumetric
 244 unfrozen water content at saturate state). Fig. 9 shows SFCC of all soils where unfrozen
 245 degree of saturation was plotted versus temperature. For each soil, from the initial saturated
 246 state, when soil temperature decreased from 0 °C, soil remained saturated with unfrozen
 247 water. When temperature reached the temperature of spontaneous nucleation, freezing was
 248 triggered inducing significant decrease of unfrozen water degree of saturation. After this step,
 249 cooling induced only slight decrease of unfrozen water degree of saturation. During the
 250 heating path, unfrozen water degree of saturation increased gradually with temperature and
 251 the relationship between these two quantities was significantly different from the cooling path
 252 for all soils.

253



254

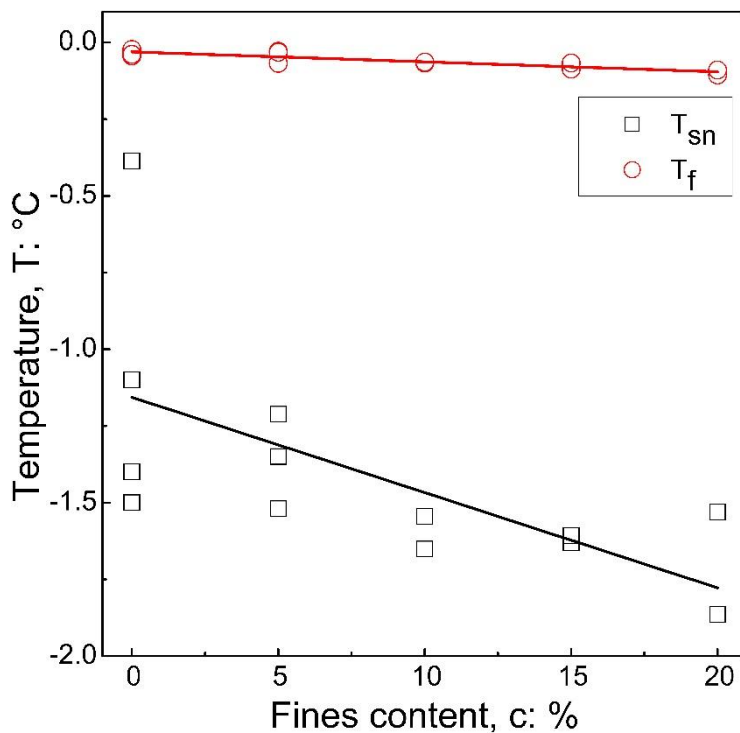
255 **Fig. 8** Soil freezing characteristic curve (volumetric unfrozen water content versus
 256 temperature) for all soils.



257

258 **Fig. 9** Soil freezing characteristic curve (unfrozen water degree of saturation versus
 259 temperature) for all soils.

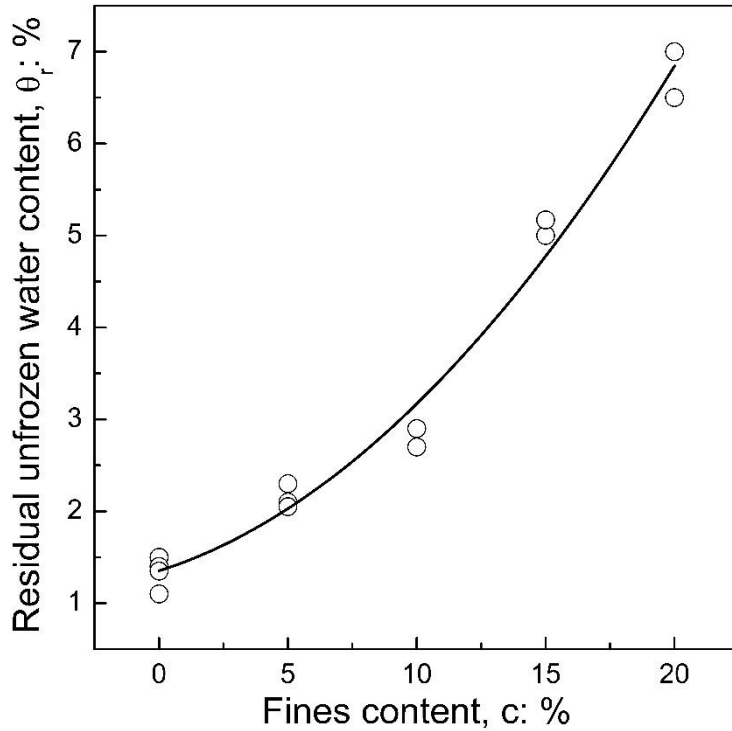
260 In order to quantitatively assess the effects of fines content, temperatures of spontaneous
 261 nucleation T_{sn} and freezing point T_f were plotted versus fines content (Fig. 10). The results
 262 show that the temperature of freezing point was close to 0 °C for all soils. The results were
 263 quite repeatable (with variation less than 0.1 °C) and only a slight trend of decrease of T_f
 264 when fines content increase could be observed. For T_{sn} , results showed a higher scattering (up
 265 to 0.5 °C, except for test at 0% of clay content where this value varied from -0.4 °C to -1.5
 266 °C). In general, T_{sn} is lower at a higher clay content.



267

268 **Fig. 10** Temperatures of spontaneous nucleation and freezing point versus fines content

269 Fig. 11 shows the residual unfrozen water content θ_r (the value determined at a temperature
 270 equal to T_{sn} , see Fig. 5) versus fines content. A good repeatability (with a scattering of 0.5 %)
 271 could be observed. The results show that residual unfrozen water content was higher at a
 272 higher fines content.



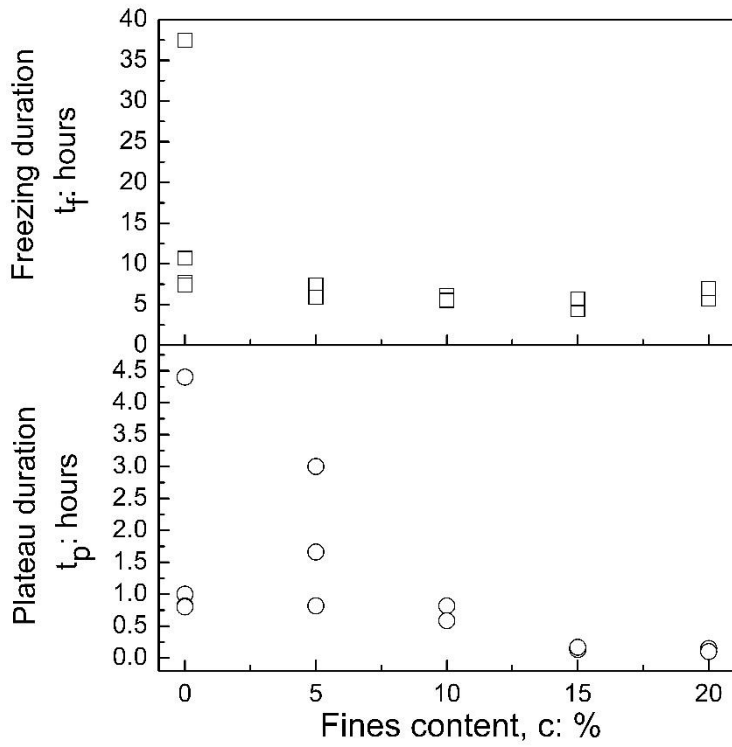
273

274 **Fig. 11** Residual unfrozen water content versus fines content.

275 Fig. 12 presents the duration of the temperature plateau t_p and the duration of the freezing
 276 process t_f (see the definition on Fig. 5) versus fines content. Results of t_p were quite scattering
 277 for 0 and 5% of fines content, varying from 0.80 to 4.40 h. They were more repeatable at
 278 higher fines contents. A general decrease of this duration when the fines contents increased
 279 could be observed. Results of t_f varied between 5 and 10 h (except one test, S0-T1 where it
 280 was very long, 37.50 h). These results did not show any clear trend.

281 Table 5 shows the obtained characteristic parameters of all tests for better comparison.

282



283

284 **Fig. 12** Duration of the temperature plateau and duration of the freezing process versus fines
 285 content.

286 Table 5: Summary of characteristic parameters in freezing of tests

Test No.	Fines content (%)	T_{sn} (°C)	T_f (°C)	θ_r (-)	t_p (h)	t_f (h)
S20-T1	20	-1.86	-0.11	6.5	0.15	5.65
S20-T2	20	-1.53	-0.09	7.0	0.10	6.95
S15-T1	15	-1.61	-0.07	5.2	0.17	5.70
S15-T2	15	-1.63	-0.09	5.0	0.13	4.00
S10-T1	10	-1.65	-0.07	2.9	0.58	5.50
S10-T2	10	-1.55	-0.06	2.7	0.80	6.10
S5-T1	5	-1.52	-0.03	2.3	0.82	5.90
S5-T2	5	-1.21	-0.07	2.1	3.10	7.35
S5-T3	5	-1.35	-0.03	2.1	1.70	7.40
S0-T1	0	-0.39	-0.04	1.5	4.40	37.50
S0-T2	0	-1.51	-0.02	1.10	1.00	7.70
S0-T3	0	-1.10	-0.04	1.40	0.80	10.70

S0-T4	0	-1.40	-0.02	1.35	0.80	7.40
-------	---	-------	-------	------	------	------

287

288 **4. Discussion**

289 In this study, in order to determine the relationship between unfrozen water content and
290 temperature during a freezing-thawing cycle, large soil specimens (150 mm in height and 150
291 mm in diameter) were prepared in order to embed several sensors within the soil mass. To
292 minimise thermal and any other gradients, soil temperature was changed by small steps and
293 equilibrium was checked at the end of each step prior the subsequent step. At equilibrium, the
294 soil temperature and unfrozen water content were thus supposed to be homogeneous within
295 the specimen. Similar large soil specimens were equally used in previous studies investigating
296 SFCC with TDR method for measurement of unfrozen water content [18, 53, 75, 78]. Smaller
297 specimens were used when measurements were performed by pulsed-NMR method [30, 63,
298 79]. In several previous works, specimens were immersed in a cooling bath with constant
299 cooling rate or at low temperature (between -15 °C and -30 °C) and kept for several hours [17,
300 73, 80, 81]. For determining SFCC, unfrozen water content was measured at various
301 controlled temperatures [18, 53, 75, 76, 78, 79]. The difference between two successive
302 controlled temperatures in these studies varies between 0.3 °C and 5 °C. In the present work,
303 temperature steps of 0.1 °C and 0.2 °C were chosen before the occurrence of freezing
304 phenomenon and afterward, respectively, in order to determine more accurately the freezing
305 point, the temperature of spontaneous nucleation and the SFCC.

306 The measurement of unfrozen water content in the present study was converted from the
307 measurement of apparent dielectric constant. In this study, under the influence of temperature,
308 dielectric constant of each phase in soils changes, particularly those of water and ice [82, 83].
309 Several models exist to estimate moisture content from unfrozen soil apparent dielectric
310 constant [51, 53, 57–60, 84–86]. The most used is Topp's empirical model [57] but it is not
311 compatible with frozen soils [44, 58, 87]. Otherwise, Smith and Tice [58] proposed a model
312 based on comparison of unfrozen water content measured from NMR and TDR methods for
313 25 soils covering a wide range of specific surface areas. For this reason, in the present work,
314 the model of Smith and Tice [58], which provides an accuracy of $\pm 3\%$ compared to
315 measurements from NMR method, was used for frozen soils.

316 Hysteresis of SFCC (difference between the freezing and the thawing curves) is usually
317 attributed to the same factors inducing hysteresis in SWCC, such as the effect of electrolytes,
318 pore geometry, pore blocking, effect of contact angle and change in pore structure [78].
319 Actually, in a freezing process, increasing solute concentration by forming ice from water
320 increases the effect of electrolyte. Otherwise, forming ice also changes soil skeleton that
321 affects matric potentials of soils. In addition, the hysteric behaviour is also mainly attributed
322 to supercooling of pore water [18, 54, 62, 63]. Instead of freezing at 0 °C, pore water is
323 necessarily supercooled at lower temperature. In the present work, an insignificant hysteresis
324 of θ_u was observed for all soils below T_{sn} (at frozen state). First, the effect of electrolytes can
325 be ignored. Second, temperature below T_{sn} of -1 °C to -2 °C corresponds to a suction of 1
326 MPa to 2.5 MPa following the Clapeyron equation. This high range of suction corresponds
327 mainly to water in micropore (intra-aggregates) in the clay matrix where SWCC is also
328 reversible. As a result, hysteresis of SFCC observed in the present work could be contributed
329 mainly to supercooling. After the triggering of freezing, SFCC obtained at temperature lower
330 than T_{sn} were generally reversible (see Fig. 8 & Fig. 9).

331 Results shown in Fig. 9 demonstrate significant effect of fines content on the thawing path of
332 SFCC; at a given temperature, a higher unfrozen water degree of saturation was obtained at a
333 higher fines content. These results are consistent with the findings of previous works [28, 55,
334 63, 70]. Following these studies, Gibbs-Thompson equation can be used to relate the pore size
335 distribution and the thawing path of SFCC; a lower temperature corresponds to a smaller pore.
336 In the present work, soil having higher fines content would have a larger volume of
337 micropores (inter-aggregates and intra-aggregates pores) a lower volume of macropores
338 (space between sand particles).

339 T_{sn} determined in this study can be associated to supercooling. Fig. 10 shows that this
340 parameter generally decreased with an increase of fines content and it was measured with a
341 relatively high scattering. For bulk water, T_{sn} depend on numerous factors such as sample
342 volume, cooling velocity, the presence and concentration of solutes, the presence of solid
343 impurities, effects of external fields (impulse waves, electromagnetic radiation, etc.) [9, 89,
344 90]. In the case of soils, additional factors can be soil components and their fractions. Many
345 studies determined T_{sn} of various soils and found that increasing clay content in soils
346 decreases temperature of spontaneous nucleation to lower range [15, 18]. These studies
347 focused on clays or clay and silt and these results agree with sandy soils in the present study.

348 It is noted that the supercooling is considered as a necessary phase to activate nucleation
349 process and it appears in both cases, either in free pure water or within the porous volume of
350 soils. Because of the high value of released latent heat, about 334 J/g, which appears during
351 nucleation process, water needs to be supercooled at T_{sn} for equilibrating energy before
352 crystallization. According to Yershov [91], T_{sn} is remarked as the temperature at which
353 embryo nuclei form and grow to the critical sizes, about 472 H₂O corresponding to 10^{-26} m³.
354 The relatively high scattering of results obtained in the present work can be thus explained by
355 the random behaviour of the crystallization process. The slight effect of fines content on T_{sn}
356 can be explained by the effect of soil pore size distribution on the supercooling: soil having a
357 higher fines content would have higher volume of micropores, and T_{sn} is generally lower in a
358 smaller pore.

359 Numerous studies investigated T_f and showed that T_f depends on many factors such as salt
360 content [20, 73, 80, 92, 93], salt types [17, 81], initial water content [15], soil types [10, 18,
361 30, 55, 94, 95], etc. In the present study, T_f was found close to 0 °C for all soils. This result
362 can be explained by two main reasons: soils were studied at saturated state and fines content
363 is sufficiently low. Bing and Ma [81] obtained similar results with saturated sandy soil
364 containing less than 7.5% of clay. Furthermore, freezing point remains constant also above a
365 certain value of water content for all soils [9, 81, 96]. Actually, for the soils considered in the
366 present study, with relatively low contents of low plasticity kaolin clay, the amount of bound
367 water should be negligible and T_f should be similar to that of bulk pure water, i.e. close to 0
368 °C.

369 Residual unfrozen content was found higher at a higher fines content (Fig. 11). It is believed
370 that residual unfrozen relates almost directly to the amount of specific surface of soils.
371 According to several studies [18, 28, 30, 55, 63], unfrozen water content remaining in soils at
372 the same temperature decreased in the following order: clay, silts, sands and gravel.
373 Following Bing and Ma [81], only free water was frozen when freezing is triggered. Unfrozen
374 water should then correspond to bound water. According to Tian et al. [63], the amount of
375 bound water in soils is proportional to the thickness of the electric double layer and specific
376 surface area. In the present study, a higher fines content corresponds to a higher specific
377 surface area and then a higher amount of bound water.

378 The duration of temperature plateau, t_p , would depend then on the amount of latent heat
379 released when freezing is triggered. This amount mainly depends on T_{sn} , as shown in Table 5.

380 As the results of T_{sn} show significant scattering and a general slight increase when fines
381 content increased (Fig. 10), similar trends were observed with t_p (Fig. 12). The duration of the
382 freezing process, t_f , which is much longer than t_p , correspond to the thermal diffusion of latent
383 heat released during the whole freezing process. This duration would depend thus mainly on
384 the thermal diffusivity of the frozen soil (which at the same time evolves during freezing).

385

386 **5. Conclusions**

387 The results obtained in this study show that fines content in sandy soils significantly
388 influenced the soil behaviour under a freezing-thawing cycle. Based on the investigation of
389 five levels of fines content (varying from 0 to 20 %), the following conclusions can be
390 addressed:

- 391 - When the temperature decreased from 0°C, freezing was triggered at T_{sn} inducing a
392 sudden decrease of θ_u from the saturated state to the residual state. Afterward, θ_u
393 continued to decrease but with a lower rate. The subsequent heating induced an
394 increase of θ_u (which represents a progressive melting of frozen water).
- 395 - The thawing path of SFCC was strongly dependent on the fines content; at a given
396 temperature, a higher θ_u was observed for a higher fines content.
- 397 - T_{sn} was higher at a higher fines content and varied between -1.0 °C and -2.0 °C.
- 398 - T_f varied between 0°C and -0.2 °C, only a slight decrease of T_f with an increase of
399 fines content was observed.
- 400 - θ_r (varied from 1 % to 7 %) was higher at a higher fines content.
- 401 - t_p was found scattering and slightly decreased when fines content increased.
- 402 - t_f was found independent of fines content.

403 The findings of the present study would be helpful to predict the soil behaviour under
404 freezing-thawing process. That would imply several applications in cold regions and also in
405 geotechnical engineering ground improvement by artificial ground freezing.

406 **Data availability**

407 The datasets generated during and/or analysed during the current study are available from the
408 corresponding author on reasonable request.

409 **Funding and Competing interests**

410 No funding was received for conducting this study.

411 The authors have no competing interests to declare that are relevant to the content of this
412 article.

413

414 **References**

415 1. Andersland OB, Ladanyi B (1994) *An Introduction to Frozen Ground Engineering*.
416 Springer Science & Business Media

417 2. Andersland OB, Ladanyi B (2004) *Frozen Ground Engineering*. John Wiley & Sons

418 3. Russo G, Corbo A, Cavuoto F, Autuori S (2015) Artificial Ground Freezing to
419 excavate a tunnel in sandy soil. Measurements and back analysis. *Tunn Undergr Sp*
420 *Technol* 50:226–238. <https://doi.org/10.1016/j.tust.2015.07.008>

421 4. Han L, Ye G, Li Y, et al (2016) In situ monitoring of frost heave pressure during cross
422 passage construction using ground-freezing method. *Can Geotech J* 53:530–539.
423 <https://doi.org/10.1139/cgj-2014-0486>

424 5. Zhang S, Sheng D, Zhao G, et al (2016) Analysis of frost heave mechanisms in a high-
425 speed railway embankment. *Can Geotech J* 53:520–529. [https://doi.org/10.1139/cgj-](https://doi.org/10.1139/cgj-2014-0456)
426 [2014-0456](https://doi.org/10.1139/cgj-2014-0456)

427 6. Yu W, Zhang T, Lu Y, et al (2020) Engineering risk analysis in cold regions: State of
428 the art and perspectives. *Cold Reg Sci Technol* 171:102963.
429 <https://doi.org/10.1016/j.coldregions.2019.102963>

430 7. Akyurt M, Zaki G, Habeebullah B (2002) Freezing phenomena in ice–water systems.
431 *Energy Convers Manag* 43:1773–1789. [https://doi.org/10.1016/S0196-8904\(01\)00129-](https://doi.org/10.1016/S0196-8904(01)00129-7)
432 [7](https://doi.org/10.1016/S0196-8904(01)00129-7)

433 8. Chen SL, Lee TS (1998) A study of supercooling phenomenon and freezing probability
434 of water inside horizontal cylinders. *Int J Heat Mass Transf* 41:769–783.

- 435 [https://doi.org/10.1016/S0017-9310\(97\)00134-8](https://doi.org/10.1016/S0017-9310(97)00134-8)
- 436 9. Kozłowski T (2009) Some factors affecting supercooling and the equilibrium freezing
437 point in soil–water systems. *Cold Reg Sci Technol* 59:25–33.
438 <https://doi.org/10.1016/j.coldregions.2009.05.009>
- 439 10. Kozłowski T (2004) Soil freezing point as obtained on melting. *Cold Reg Sci Technol*
440 38:93–101. <https://doi.org/10.1016/j.coldregions.2003.09.001>
- 441 11. Mishima O, Stanley HE (1998) The relationship between liquid, supercooled and
442 glassy water. *Nature* 396:329–335. <https://doi.org/10.1038/24540>
- 443 12. Enniful HRNB, Schneider D, Kohns R, et al (2020) A novel approach for advanced
444 thermoporometry characterization of mesoporous solids: Transition kernels and the
445 serially connected pore model. *Microporous Mesoporous Mater* 309:110534.
446 <https://doi.org/10.1016/j.micromeso.2020.110534>
- 447 13. Schreiber A, Ketelsen I, Findenegg GH (2001) Melting and freezing of water in
448 ordered mesoporous silica materials. *Phys Chem Chem Phys* 3:1185–1195.
449 <https://doi.org/10.1039/b010086m>
- 450 14. Petrov O, Furó I (2006) Curvature-dependent metastability of the solid phase and the
451 freezing-melting hysteresis in pores. *Phys Rev E* 73:011608.
452 <https://doi.org/10.1103/PhysRevE.73.011608>
- 453 15. Anderson DM (1968) Undercooling, freezing point depression, and ice nucleation of
454 soil water. *Isr J Chem* 6:349–355. <https://doi.org/10.1002/ijch.196800044>
- 455 16. ANDERSON DM (1967) Ice nucleation and the substrate-ice interface. *Nature*
456 216:563–566. <https://doi.org/10.1038/216563a0>
- 457 17. Wan X, Lai Y, Wang C (2015) Experimental study on the freezing temperatures of
458 saline silty soils. *Permafr Periglac Process* 26:175–187.
459 <https://doi.org/10.1002/ppp.1837>
- 460 18. Zhang M, Zhang X, Lai Y, et al (2020) Variations of the temperatures and volumetric
461 unfrozen water contents of fine-grained soils during a freezing–thawing process. *Acta*

- 462 Geotech 15:595–601. <https://doi.org/10.1007/s11440-018-0720-z>
- 463 19. Yu F, Guo P, Na S (2022) A framework for constructing elasto- plastic constitutive
464 models for frozen and unfrozen soils. *Int J Numer Anal Methods Geomech* 46:436–
465 466. <https://doi.org/10.1002/nag.3306>
- 466 20. Ayers AD, Campell RB (1951) Freezing point of water in a soil as related to salt and
467 moisture contents of the soil. *Soil Sci* 72:201–206
- 468 21. He Z, Teng J, Yang Z, et al (2020) An analysis of vapour transfer in unsaturated
469 freezing soils. *Cold Reg Sci Technol* 169:102914.
470 <https://doi.org/10.1016/j.coldregions.2019.102914>
- 471 22. Teng J, Zhong Y, Zhang S, Sheng D (2021) A mathematic model for the soil freezing
472 characteristic curve: the roles of adsorption and capillarity. *Cold Reg Sci Technol*
473 181:103178. <https://doi.org/10.1016/j.coldregions.2020.103178>
- 474 23. Anderson DM, Tice AR (1972) Predicting unfrozen water contents in frozen soils from
475 surface area measurements. *Highw Res Rec* 393:12–18
- 476 24. Kozlowski T (2007) A semi-empirical model for phase composition of water in clay–
477 water systems. *Cold Reg Sci Technol* 49:226–236.
478 <https://doi.org/10.1016/j.coldregions.2007.03.013>
- 479 25. Kozlowski T, Nartowska E (2013) Unfrozen Water Content in Representative
480 Bentonites of Different Origin Subjected to Cyclic Freezing and Thawing. *Vadose Zo J*
481 12:. <https://doi.org/10.2136/vzj2012.0057>
- 482 26. Ye M, Pan F, Wu Y-S, et al (2007) Assessment of radionuclide transport uncertainty in
483 the unsaturated zone of Yucca Mountain. *Adv Water Resour* 30:118–134.
484 <https://doi.org/10.1016/j.advwatres.2006.03.005>
- 485 27. Ge S, McKenzie J, Voss C, Wu Q (2011) Exchange of groundwater and surface-water
486 mediated by permafrost response to seasonal and long term air temperature variation.
487 *Geophys Res Lett* 38:1–6. <https://doi.org/10.1029/2011GL047911>
- 488 28. Tice AR, Anderson DM, Banin A (1976) The prediction of unfrozen water contents in

- 489 frozen soils from liquid limit determinations. Department of Defense, Army, Corps of
490 Engineers, Cold Regions Research and Engineering Laboratory
- 491 29. Dall'Amico M (2010) Coupled water and heat transfer in permafrost modeling.
492 University of Trento
- 493 30. Teng J, Kou J, Yan X, et al (2020) Parameterization of soil freezing characteristic
494 curve for unsaturated soils. *Cold Reg Sci Technol* 170:102928.
495 <https://doi.org/10.1016/j.coldregions.2019.102928>
- 496 31. Zhang X, Sun SF, Xue Y (2007) Development and Testing of a Frozen Soil
497 Parameterization for Cold Region Studies. *J Hydrometeorol* 8:690–701.
498 <https://doi.org/10.1175/JHM605.1>
- 499 32. Sheshukov AY, Nieber JL (2011) One-dimensional freezing of nonheaving unsaturated
500 soils: Model formulation and similarity solution. *Water Resour Res* 47:1–17.
501 <https://doi.org/10.1029/2011WR010512>
- 502 33. Liu Z, Yu X (Bill) (2013) Physically Based Equation for Phase Composition Curve of
503 Frozen Soils. *Transp Res Rec J Transp Res Board* 2349:93–99.
504 <https://doi.org/10.3141/2349-11>
- 505 34. Zhang S, Teng J, He Z, et al (2016) Canopy effect caused by vapour transfer in covered
506 freezing soils. *Géotechnique* 66:927–940. <https://doi.org/10.1680/jgeot.16.P.016>
- 507 35. Zhou Y, Zhou J, Shi X, Zhou G (2019) Practical models describing hysteresis behavior
508 of unfrozen water in frozen soil based on similarity analysis. *Cold Reg Sci Technol*
509 157:215–223. <https://doi.org/10.1016/j.coldregions.2018.11.002>
- 510 36. Sun K, Zhou A (2021) A multisurface elastoplastic model for frozen soil. *Acta Geotech*
511 16:3401–3424. <https://doi.org/10.1007/s11440-021-01391-7>
- 512 37. Kebria MM, Na S, Yu F (2022) An algorithmic framework for computational
513 estimation of soil freezing characteristic curves. *Int J Numer Anal Methods Geomech*
514 46:1544–1565. <https://doi.org/10.1002/nag.3356>
- 515 38. Watanabe K, Mizoguchi M (2002) Amount of unfrozen water in frozen porous media

- 516 saturated with solution. *Cold Reg Sci Technol* 34:103–110.
517 [https://doi.org/10.1016/S0165-232X\(01\)00063-5](https://doi.org/10.1016/S0165-232X(01)00063-5)
- 518 39. Zhou J, Wei C, Lai Y, et al (2018) Application of the Generalized Clapeyron Equation
519 to Freezing Point Depression and Unfrozen Water Content. *Water Resour Res*
520 54:9412–9431. <https://doi.org/10.1029/2018WR023221>
- 521 40. Ishizaki T, Maruyama M, Furukawa Y, Dash J (1996) Premelting of ice in porous silica
522 glass. *J Cryst Growth* 163:455–460
- 523 41. Bai R, Lai Y, Zhang M, Yu F (2018) Theory and application of a novel soil freezing
524 characteristic curve. *Appl Therm Eng* 129:1106–1114.
525 <https://doi.org/10.1016/j.applthermaleng.2017.10.121>
- 526 42. Koopmans RWR, Miller RD (1966) Soil freezing and soil water characteristic curves.
527 *Soil Sci Soc Am J* 30:680–685
- 528 43. Patterson DE, Smith MW (1981) The measurement of unfrozen water content by time
529 domain reflectometry: results from laboratory tests. *Can Geotech J* 18:131–144.
530 <https://doi.org/10.1139/t81-012>
- 531 44. Spaans EJ a, Baker JM (1995) Examining the use of time domain reflectometry for
532 measuring liquid water content in frozen soil. *Water Resour Res* 31:2917–2925.
533 <https://doi.org/10.1029/95WR02769>
- 534 45. Anderson DM, Tice AR (1973) The unfrozen interfacial phase in frozen soil water
535 systems. In: *Physical aspects of soil water and salts in ecosystems*. pp 107–124
- 536 46. Kolaian JH, Low PF (1963) Calorimetric determination of unfrozen water in
537 montmorillonite pastes. *Soil Sci* 95:376–384
- 538 47. Kozlowski T (2003) A comprehensive method of determining the soil unfrozen water
539 curves. *Cold Reg Sci Technol* 36:71–79. [https://doi.org/10.1016/S0165-232X\(03\)00007-7](https://doi.org/10.1016/S0165-232X(03)00007-7)
540
- 541 48. Yong RN, Cheung C, Sheeran DE (1979) Prediction of Salt Influence on Unfrozen
542 Water Content in Frozen Soils. In: *Developments in Geotechnical Engineering*. pp

543 137–155

- 544 49. Anderson DM, Hoekstra P (1965) Migration of interlamellar water during freezing and
545 thawing of Wyoming bentonite. *Soil Sci Soc Am J* 29:498–504.
546 <https://doi.org/10.2136/sssaj1965.03615995002900050010x>
- 547 50. Anderson DM, Morgenstern NR (1973) Physics, chemistry, and mechanics of frozen
548 ground: a review. In: *Permafrost: North American Contribution [to The] Second*
549 *International Conference; National Academies: Washington, DC, USA.* p 257
- 550 51. Stähli M, Stadler D (1997) Measurement of water and solute dynamics in freezing soil
551 columns with time domain reflectometry. *J Hydrol* 195:352–369.
552 [https://doi.org/10.1016/S0022-1694\(96\)03227-1](https://doi.org/10.1016/S0022-1694(96)03227-1)
- 553 52. Zhou X, Zhou J, Kinzelbach W, Stauffer F (2014) Simultaneous measurement of
554 unfrozen water content and ice content in frozen soil using gamma ray attenuation and
555 TDR. *J Am Water Resour Assoc* 5:2–2. [https://doi.org/10.1111/j.1752-](https://doi.org/10.1111/j.1752-1688.1969.tb04897.x)
556 [1688.1969.tb04897.x](https://doi.org/10.1111/j.1752-1688.1969.tb04897.x)
- 557 53. Schafer H, Beier N (2020) Estimating soil-water characteristic curve from soil-freezing
558 characteristic curve for mine waste tailings using time domain reflectometry. *Can*
559 *Geotech J* 57:73–84. <https://doi.org/10.1139/cgj-2018-0145>
- 560 54. Tice AR, Anderson DM, Sterrett KF (1982) Unfrozen water contents of submarine
561 permafrost determined by nuclear magnetic resonance. In: *Developments in*
562 *Geotechnical Engineering.* pp 135–146
- 563 55. Li Z, Chen J, Sugimoto M (2020) Pulsed NMR Measurements of Unfrozen Water
564 Content in Partially Frozen Soil. *J Cold Reg Eng* 34:04020013.
565 [https://doi.org/10.1061/\(ASCE\)CR.1943-5495.0000220](https://doi.org/10.1061/(ASCE)CR.1943-5495.0000220)
- 566 56. Yoshikawa K, Overduin PP (2005) Comparing unfrozen water content measurements
567 of frozen soil using recently developed commercial sensors. *Cold Reg Sci Technol*
568 42:250–256. <https://doi.org/10.1016/j.coldregions.2005.03.001>
- 569 57. Topp GC, Davis JL, Annan AP (1980) Electromagnetic determination of soil water
570 content: Measurements in coaxial transmission lines. *Water Resour Reserch* 16:574–

571 582

- 572 58. Smith MW, Tice AR (1988) Measurement of the unfrozen water content of soils:
573 comparison of NMR and TDR methods. CRREL report, 88 - 18.
- 574 59. Roth K, Schulin R, Fluhler H, Attinger W (1990) Calibration of time domain
575 reflectometry for water content measurement using a composite dielectric approach.
576 WATER Resour Res VOL 26:2267–2273
- 577 60. Watanabe K, Wake T (2009) Measurement of unfrozen water content and relative
578 permittivity of frozen unsaturated soil using NMR and TDR. Cold Reg Sci Technol
579 59:34–41. <https://doi.org/10.1016/j.coldregions.2009.05.011>
- 580 61. Spaans EJA, Baker JM (1996) The Soil Freezing Characteristic: Its Measurement and
581 Similarity to the Soil Moisture Characteristic. Soil Sci Soc Am J 60:13–19
- 582 62. Bittelli M, Flury M, Campbell GS (2003) A thermodielectric analyzer to measure the
583 freezing and moisture characteristic of porous media. Water Resour Res 39:
- 584 63. Tian H, Wei C, Wei H, Zhou J (2014) Freezing and thawing characteristics of frozen
585 soils: Bound water content and hysteresis phenomenon. Cold Reg Sci Technol 103:74–
586 81. <https://doi.org/10.1016/j.coldregions.2014.03.007>
- 587 64. Horiguchi K, Miller RD (1980) Experimental studies with frozen soil in an “ice
588 sandwich” permeameter. Cold Reg Sci Technol 3:177–183.
589 [https://doi.org/10.1016/0165-232X\(80\)90023-3](https://doi.org/10.1016/0165-232X(80)90023-3)
- 590 65. Kruse AM, Darrow MM (2017) Adsorbed cation effects on unfrozen water in fine-
591 grained frozen soil measured using pulsed nuclear magnetic resonance. Cold Reg Sci
592 Technol 142:42–54. <https://doi.org/10.1016/j.coldregions.2017.07.006>
- 593 66. Hu G, Zhao L, Zhu X, et al (2020) Review of algorithms and parameterizations to
594 determine unfrozen water content in frozen soil. Geoderma 368:114277.
595 <https://doi.org/10.1016/j.geoderma.2020.114277>
- 596 67. Hoekstra P (1966) Moisture movement in soils under temperature gradients with the
597 cold-side temperature below freezing. Water Resour Res 2:241–250

- 598 68. Torrance JK, Schellekens FJ (2006) Chemical factors in soil freezing and frost heave.
599 Polar Rec (Gr Brit) 42:33–42. <https://doi.org/10.1017/S0032247405004894>
- 600 69. Arenson LU, Johansen MM, Springman SM (2004) Effects of volumetric ice content
601 and strain rate on shear strength under triaxial conditions for frozen soil samples.
602 Permafrost Periglacial Process 15:261–271. <https://doi.org/10.1002/ppp.498>
- 603 70. Zhang H, Zhang J, Zhang Z, et al (2020) Variation behavior of pore-water pressure in
604 warm frozen soil under load and its relation to deformation. Acta Geotechnica 15:603–614.
605 <https://doi.org/10.1007/s11440-018-0736-4>
- 606 71. Darrow MM (2011) Thermal modeling of roadway embankments over permafrost.
607 Cold Regions Science and Technology 65:474–487. <https://doi.org/10.1016/j.coldregions.2010.11.001>
- 608 72. Mu QY, Zhou C, Ng CWW, Zhou GGD (2019) Stress Effects on Soil Freezing
609 Characteristic Curve: Equipment Development and Experimental Results. Vadose Zone Journal
610 18:1–10. <https://doi.org/10.2136/vzj2018.11.0199>
- 611 73. Ming F, Chen L, Li D, Du C (2020) Investigation into Freezing Point Depression in
612 Soil Caused by NaCl Solution. Water 12:2232. <https://doi.org/10.3390/w12082232>
- 613 74. Suzuki S (2004) Dependence of unfrozen water content in unsaturated frozen clay soil
614 on initial soil moisture content. Soil Science and Plant Nutrition 50:603–606.
615 <https://doi.org/10.1080/00380768.2004.10408518>
- 616 75. Wu M, Tan X, Huang J, et al (2015) Solute and water effects on soil freezing
617 characteristics based on laboratory experiments. Cold Regions Science and Technology 115:22–29.
618 <https://doi.org/10.1016/j.coldregions.2015.03.007>
- 619 76. Jia H, Ding S, Wang Y, et al (2019) An NMR-based investigation of pore water
620 freezing process in sandstone. Cold Regions Science and Technology 168:102893.
621 <https://doi.org/10.1016/j.coldregions.2019.102893>
- 622 77. Boussaid K (2005) Sols intermédiaires pour la modélisation physique : application aux
623 fondations superficielles. École Centrale de Nantes et Université de Nantes
- 624 78. Ren J, Vanapalli SK (2019) Comparison of Soil- Freezing and Soil- Water

- 625 Characteristic Curves of Two Canadian Soils. *Vadose Zo J* 18:1–14.
626 <https://doi.org/10.2136/vzj2018.10.0185>
- 627 79. Ma T, Wei C, Xia X, et al (2017) Soil freezing and soil water retention characteristics:
628 connection and solute effects. *J Perform Constr Facil* 31:1–8.
629 [https://doi.org/10.1061/\(ASCE\)CF.1943-5509.0000851](https://doi.org/10.1061/(ASCE)CF.1943-5509.0000851)
- 630 80. Wan X, Liu E, Qiu E (2021) Study on ice nucleation temperature and water freezing in
631 saline soils. *Permafr Periglac Process* 32:119–138. <https://doi.org/10.1002/ppp.2081>
- 632 81. Bing H, Ma W (2011) Laboratory investigation of the freezing point of saline soil.
633 *Cold Reg Sci Technol* 67:79–88. <https://doi.org/10.1016/j.coldregions.2011.02.008>
- 634 82. Wraith JM, Or D (1999) Temperature effects on soil bulk dielectric permittivity
635 measured by time domain reflectometry: Experimental evidence and hypothesis
636 development. *Water Resour Res* 35:361–369
- 637 83. Haynes WM (2016) *CRC Handbook of Chemistry and Physics*, 97th Editi. CRC press
- 638 84. Birchak JR, Gardner CG, Hipp JE, Victor JM (1974) High dielectric constant
639 microwave probes for sensing soil moisture. *Proc IEEE* 62:93–98.
640 <https://doi.org/10.1109/PROC.1974.9388>
- 641 85. He H, Dyck M (2013) Application of multiphase dielectric mixing models for
642 understanding the effective dielectric permittivity of frozen soils. *Vadose Zo J* 12:.
643 <https://doi.org/10.2136/vzj2012.0060>
- 644 86. Nagare RM, Schincariol RA, Quinton WL, Hayashi M (2011) Laboratory calibration of
645 time domain reflectometry to determine moisture content in undisturbed peat samples.
646 *Eur J Soil Sci* 62:505–515. <https://doi.org/10.1111/j.1365-2389.2011.01351.x>
- 647 87. Zhou X, Zhou J, Kinzelbach W, Stauffer F (2014) Simultaneous measurement of
648 unfrozen water content and ice content in frozen soil using gamma ray attenuation and
649 TDR. *Water Resour Res* 50:9630–9655. <https://doi.org/10.1002/2014WR015640>
- 650 88. Su Y, Cui Y-J, Dupla J-C, Canou J (2022) Soil-water retention behaviour of fine/coarse
651 soil mixture with varying coarse grain contents and fine soil dry densities. *Can Geotech*

- 652 J 59:291–299. <https://doi.org/10.1139/cgj-2021-0054>
- 653 89. Fletcher NH (1970) *The chemical physics of ice*. Press Cambridge, Engl 111
- 654 90. Y.Uzu, Sano I (1965) On the Freezing of the Droplets of Aqueous Solutions. *J*
655 *Meteorol Soc Japan Ser II* 43:290–292
- 656 91. Yershov ED (2004) *General Geocryology*. Cambridge University Press
- 657 92. Banin A, Anderson DM (1974) Effects of Salt Concentration Changes During Freezing
658 on the Unfrozen Water Content of Porous Materials. *Water Resour Res* 10:124–128
- 659 93. Han Y, Wang Q, Kong Y, et al (2018) Experiments on the initial freezing point of
660 dispersive saline soil. *Catena* 171:681–690.
661 <https://doi.org/10.1016/j.catena.2018.07.046>
- 662 94. Cannell GH, Gardner WH (1959) Freezing-point depressions in stabilized soil
663 aggregates, synthetic soil, and quartz sand. *Soil Sci Soc Am J* 23:418–422.
664 <https://doi.org/10.2136/sssaj1959.03615995002300060018x>
- 665 95. Kozłowski T (2016) A simple method of obtaining the soil freezing point depression,
666 the unfrozen water content and the pore size distribution curves from the DSC peak
667 maximum temperature. *Cold Reg Sci Technol* 122:18–25.
668 <https://doi.org/10.1016/j.coldregions.2015.10.009>
- 669 96. Wen Z, Ma W, Feng W, et al (2012) Experimental study on unfrozen water content and
670 soil matric potential of Qinghai-Tibetan silty clay. *Environ Earth Sci* 66:1467–1476.
671 <https://doi.org/10.1007/s12665-011-1386-0>

672

673

674